Development of Precise Point Positioning Algorithm to Support Advanced Driver Assistant Functions for Inland Vessel Navigation

C. Lass & R. Ziebold
German Aerospace Centre (DLR), Neustrelitz, Germany

ABSTRACT: Bridge passing and passing waterway locks are two of the most challenging phases for inland vessel navigation. In order to be able to automate these critical phases very precise and reliable position, navigation and timing (PNT) information are required. Here, the application of code-based positioning using signals of Global Navigation Satellite Systems (GNSS) is not sufficient anymore and phase-based positioning needs to be applied. Due to the larger coverage area and the reduction of the amount of correction data Precise Point Positioning (PPP) has significant advantages compared to the established Real Time Kinematic (RTK) positioning. PPP is seen as the key enabler for highly automatic driving for both road and inland waterway transport. This paper gives an overview of the current status of the developments of the PPP algorithm, which should finally be applied in advanced driver assistant functions. For the final application State Space Representation (SSR) correction data from SAPOS (Satellitenpositionierungsdienst der deutschen Landesvermessung) will be used, which will be transmitted over VDES (VHF Data Exchange System), the next generation AIS.

1 INTRODUCTION

Inland shipping is an important pillar of the European transport system. Nevertheless, it needs to compete with other modes of transport like road and rail transport. In order to increase both efficiency and safety of inland navigation, advanced driver assistant functions are currently being developed. Two of the most challenging phases of inland navigation are the bridge passing and the passing of waterway locks. For the entering of a waterway lock typically a vessel with a width of 11.4 m and a length of 100 m (or even 200 m) needs to pass a 12 m wide lock chamber. This results in very tight requirements for the determination of position, heading and velocity of the vessel. Bridge passing additionally yields to tight requirements on the height determination, namely 10 cm [5].

In order to reach these accuracies, phase-based positioning needs to be applied. One can distinguish between relative positioning by means of RTK (Real Time Kinematic) using correction data of a nearby real or virtual reference station and absolute positioning by means of PPP (Precise Point Positioning) using corrections from a global network of reference stations. PPP [20] enables accurate positioning for a single receiver without the need for differential techniques by modelling and correcting for the different error sources. State-of-the-art algorithms such as the Canadian Spatial Reference System Precise Point Positioning (CSRS-PPP) of the Canadian Geodetic Survey of Natural Resources Canada [17] can be freely used to analyse measurements in postprocessing and to have an accurate reference. On the 20th of October 2020 it was upgraded to version 3

and since then allows for ambiguity resolution for data collected on or after 1st of January 2018.

For real-time application other methods have to be applied. Here, the convergence time is of upmost importance as we cannot wait an hour for the float ambiguities to converge before beginning operation. This can be achieved by PPP-RTK [19] which uses PPP based on a network of local reference stations like in RTK to derive the real-time corrections, so called State Space Representation (SSR) correction data, of individual error components like satellite clock and orbit, tropospheric and ionospheric errors as well as code and phase biases. Due to accounting for the ionospheric delay, one can use the undifferenced code and phase observations with true integer ambiguities which can be fixed without requiring a long time to converge [10]. This enables horizontal positioning close to sub-cm level in a multi-GNSS scenario [9]. An example of a nationwide PPP-RTK service is the Centimeter Level Augmentation Service (CLAS) of Japan's Quasi-Zenith Satellite System (QZSS) which provides corrections via QZS L6 signals. CLAS was upgraded on the 30th of November 2020 with a new atmospheric correction message.

Due to the fact that the service area is significantly enlarged for PPP-RTK (100-1000 km) compared to RTK (1-20 km) while also requiring a smaller data rate, PPP-RTK is seen as the key enabler for highly automatic driving for both road and inland waterway transport. The project SCIPPPER (2018-2021) aims the application of PPP-RTK for the automatic entering/exiting of a waterway lock [13]. This is a pilot project for the usage of SSR corrections provided by the SAPOS (Satellitenpositionierungsdienst der deutschen Landesvermessung) reference station network. The correction data will be broadcasted by using the new communication channel of VDES [6, 11] (VHF Data Exchange System) – the next generation of the AIS (Automatic Identification System). As the decoding of the SSR corrections in the proprietary SSRZ format [10] is in development, we will present a PPP algorithm using methods which can also be applied or easily adapted to the real-time PPP-RTK case.

The paper is organised as follows: In section 2 we discuss the driver assistant functions and their requirement on the position, navigation and timing. Afterwards, section 3 explains the associated system design. In section 4 we describe the PPP algorithm and will also put emphasis on accurate velocity estimation. The algorithm is then applied to an inland water measurement campaign which is disseminated in section 5. The final section summarises the paper and gives outlook to further activities associated with the SCIPPPER project.

2 REQUIREMENTS ON PNT PROVISION FOR DRIVER ASSISTANT FUNCTIONS

Unlike the maritime domain, where the requirements for radio-navigation systems have been clearly defined by the International Maritime Organization (IMO) [11] [12], the navigational specifications for inland waterway scenarios have not been addressed by any international committee. Therefore, the requirements for the provision of the position, navigation and timing (PNT) data have to be derived from the functional requirements of the different driver assistant functions. In [5] this has been done for assistant functions like the bridge-collision warning system, automatic guidance and the mooring assistant. For the automatic entering of a waterway lock these requirements have been deduced in the SCIPPPER project and shall be described here.

For the development of the requirements typical dimensions of the waterway lock and the inland vessel are assumed. In Figure 1 a true to scale sketch of the lock chamber together with the inland vessel is shown. The narrow gap between the vessel and the lock chamber of ideally 30 cm on both sides is hardly visible.
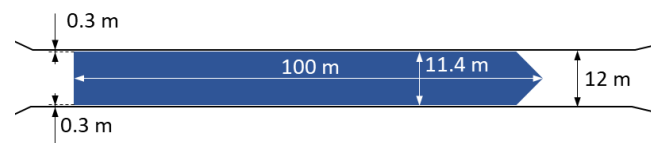
Figure 1. True to scale sketch of a typical lock chamber and inland vessel (ship width: W = 11.4 m, ship length: L = 100 m, chamber width: 12 m)

The accuracy requirements for the provision of position, velocity and orientation differ for the different phases of an automated passing of a waterway lock. At the beginning of the manoeuvre, there is more space available for manoeuvres in the outer harbour of the lock than at the time of the manoeuvre when the vessel is fully inside the lock chamber. In order to adapt the accuracy requirements to the available manoeuvring space, the entry and exit manoeuvres shall be divided into five phases as can also be seen in Figure 2:

– Phase 1: Start of the manoeuvre in the outer harbour, alignment of the position and orientation of the vessel with the lock gate or the central axis of the lock, approach in the direction of the lock gate.
– Phase 2: Achieving the required position and orientation accuracy before the actual entry into the lock. If the accuracy is not reached at the end of phase 2, an alarm is issued. The skipper must then abort the manoeuvre and take over control completely.
– Phase 3: Passing through the lock gate, manoeuvring in the lock chamber, stopping the ship.
– Phase 4: Exit from the lock.
– Phase 5: Manoeuvring in the outer harbour, taking over of control by the skipper or stopping.
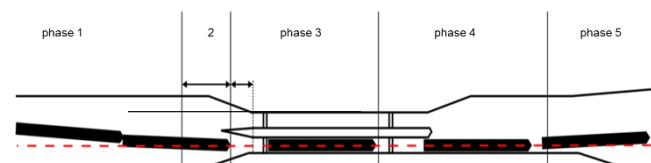
Figure 2. Schematic overview of the different phases of passing a waterway lock

The resulting accuracies for the position, heading, rate of turn (ROT) and velocity are summarised in

Table 1. The numbers have been derived by allocation of the available space between the measurement system and the control system with its actuators.

Table 1. Requirements on PNT provision for the different phases of passing a waterway lock

	Phase 1,5	Phase 2	Phase 3, 4
Horizontal positioning accuracy [cm]	10	1 (Bow), 10 (Stern)	1
Heading accuracy [°] L=100m	11°/L(m) 0.1°	11°/L(m) 0.1°	0.5°/L(m) 0.005°
ROT[°/min]	0.3	0.3	0.3
Velocity [cm/s]	1	1	1

The highest position accuracies of 1 cm are required when the whole vessel (phase 3,4) or parts of the vessel like the bow in phase 2 are in the lock chamber. Here, the shadowing and multipath of satellite signals by the up to 30 m high metallic walls like in the locks in the Main Danube Channel, will jeopardise satellite-based positioning. Therefore, close-range sensors, like LIDAR, are required here on bow and stern for local positioning in the lock chamber. The focus of this paper lies in the pure GNSS based PNT provision. The according requirements for GNSS based positioning can be found in the phases 1 and 5. Besides the high accuracy of 10 cm for the position, also the tight requirements for heading and rate of turn (ROT) and velocity need to be mentioned. The required heading accuracy scales with the length of the vessel and results in 0.1° for a length of 100 m and 0.05° for 200 m. This is one order of magnitude tighter than accuracies achievable by state of the art GNSS compass systems used on inland vessels so far. Due to the fact, that the controller for rudder, engine and thrusters mainly controls the very low longitudinal and transversal speed at bow and stern the measurement accuracy of the velocities is also of upmost importance. The required 1 cm/s is a demanding target.

Table 2. Requirements for GNSS based determination of position, height, heading and velocity for the different assistant functions developed in the projects LAESSI [5] and SCIPPPER [13]

	Lock entering (GNSS only)	Bridge-height warning	Mooring assistance	Automatic guidance
Horizontal positioning accuracy [cm]	10	20	10	30
Height accuracy [cm]	-	10	-	-
Heading accuracy [°] L=100m	11°/L(m) 0.1°	0.3°	0.07°	0.1°
Velocity [cm/s]	1	-	-	-

Table 2 summarises the different requirements for GNSS based PNT provision for the different driver assistant functions. The most stringent requirements concerning positioning of 10 cm arises from the lock entering and the mooring assistance. As expected the bridge height warning is the only assistant function with tight requirements on the height. Due to the fact, that for the lock entering not only the rudder angle but also the engine and thrusters have to be steered it is the only assistant function which requires highly accurate velocity measurements. For all assistant functions the heading accuracy is very important.

3 SYSTEM DESIGN FOR PNT PROVISION

Figure 3 gives an overview of the system design for the driver assistance functions. It can be divided into the three segments: i) shore side services, ii) onboard systems and iii) the communication link. While this paper focusses on the GNSS based PNT provision, for reasons of completeness in the figure also the other modules relevant for the driver assistant functions are shown. These are the waterway information (mainly from waterway locks) and the onboard system with the control system together with the nautical display and the closed range sensors.
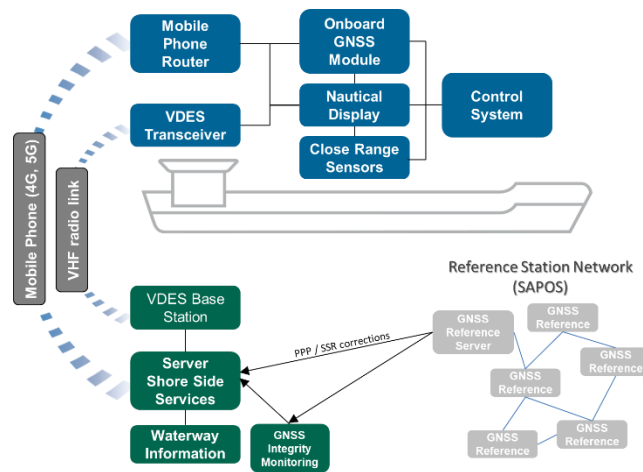
Figure 3. Schematic overview of system concept for the driver assistance function

3.1 *Shore side service*

For the GNSS based PNT provision the reference station network of the Surveying Authorities of the Laender of the Federal Republic of Germany is used. For the surveyors they provide as a standard product a network solution for the provision of virtual reference station correction for RTK positioning. As a pilot project in individual regions like Bavaria the same reference station network is used to provide SSR corrections to enable PPP positioning in the service area. Transmission of SSR correction data requires less capacity than RTK corrections and can be applied in a larger region. Thus, this is the ideal candidate for a broadcast service on a carrier with limited bandwidth. The shore side service is complemented by Integrity monitoring station and the server for shore side services which sends the SSR correction data together with the integrity information to the vessels by using the communication link.

Unfortunately, the standardisation of all required SSR correction within RTCM is still pending. Only corrections for satellites clocks and orbits as well as the code biases are described in the current RTCM

Standard 10403.3 in section 3.5.13. Therefore, the standardisation of the corrections for the tropospheric delay, the ionospheric delay and the phase biases are not finalised yet. In the SCIPPPER project the corrections are designed in the proprietary SSRZ format [4] by Geo++ which is flexible and compact but complex to decode. The content of the SSR correction data will be described in more detail in section 4.

3.2 *Communication link*

For the communication the transmission capabilities of the new VDE system (VDES) will be used together with the mobile internet connection. One part of the new VDE system is a high-speed data channel with 100 kHz bandwidth on the VHF transmission side. This data channel will be used to broadcast PPP correction data. Combining the high-speed data channel with the reduced bandwidth requirements of PPP may generate a precision navigation service that has the potential to significantly enhance accuracy of navigation on inland waterways.

3.3 *Onboard systems*

The onboard system for the GNSS based PNT provision consists of a VDES transceiver together with a mobile internet router for the reception of the SSR correction data, a setup of two GNSS antennas + receivers and an inertial measurement unit (IMU). The two GNSS antennas will be placed on the bow and stern respectively. This setup enables on the one hand the realisation of the high heading accuracy which scales with the length of the vessel. On the other hand, it should help to improve the continuity of the positioning while passing a waterway bridge. Assuming a vessel with a length of 100 m the GNSS antenna on the stern still receives signals from all satellites while the bow antenna is under the bridge and vice versa. The aim of the IMU is the provision of a short-term backup mainly for the orientation (heading) of the vessel but also for the positioning.

4 PPP ALGORITHM DEVELOPMENT

4.1 *Problem formulation*

For PPP we consider both code and phase observations with regards to frequency f_i and satellite s.

$$
\begin{aligned}
R_{i,s} &= x - x_{s2} + c\left(\delta t - \delta t_s\right) + T_s + I_{i,s} + \varepsilon_{i,s} \\
\Phi_{i,s} &= x - x_{s2} + c\left(\delta t - \delta t_s\right) + T_s - I_{i,s} + \lambda_{i,s}\left(A_{i,s} + w_s\right) + \epsilon_{i,s}
\end{aligned}
\tag{1}
$$

The variables are the receiver position x, satellite position x_s, speed of light c, receiver clock offset δt depending on which GNSS satellite s belongs to, satellite clock offset δt_s depending on satellite s, tropospheric delay T_s, ionospheric delay I_s, wave length λ_i, phase wind-up w, integer ambiguity A_i and the remaining errors $\varepsilon_{i,s}$, $\epsilon_{i,s}$ such as multipath and receiver noise.

To fulfill the requirements derived in section 2 we need precise satellite position information as well as correction data for the different error sources associated with the GNSS signals. For real-time applications, we use SSR corrections [4] which consist of

− Orbit corrections, every 30 s
− Clock corrections, every 5 s
− Ionosphere and troposphere delays, every 30 s
− Code and phase biases, every 30 s

The orbit and clock corrections refer to a specific broadcast ephemeris and are given as coefficients of a linear (orbit) and a quadratic (clock) polynomial, respectively. The issue of data of the broadcast ephemeris (IODE) can be found in the header of the orbit correction.

The SSR messages also contain an epoch time (GPS seconds of week or GLONASS seconds of day) and an update interval which define the optimal time frame the corrections should be applied. First tests showed that the corrections are received with a positive delay. Hence, old corrections, i.e. the time of application does not lie in the optimal time frame, have to be applied. This necessitates managing the corrections as well as the broadcast ephemeris they refer to. Also, a warning flag should be given if the correction is considered too old so that the observation can be downweighted or even discarded.

As the decoding for the compact but complex SSRZ format [4] is in development, a postprocessing PPP algorithm was developed which can be used or adapted to the real-time case. Hence, all methods derived here are with real-time application in mind and will use as little postprocessing knowledge as possible.

The following corrections are used in our algorithm:
− Precise satellite orbits and clocks from final products (IGS, GFZ)
− Satellite antenna phase center offset and variation (IGS)
− Tide displacements caused by sun and moon
− Phase windup

For postprocessing we use the ionosphere-free linear combination of (1) and separate the tropospheric delay into the dry (hydrostatic) and wet zenith delay Z_h, Z_w. The zenith delays are used in conjunction with Vienna mapping functions m_h, m_w [2] which depend on the elevation of satellite s, the receiver position and the time. All in all, we have:

$$
\begin{aligned}
(\cdot)_{IF} &= \frac{f_1^2(\cdot)_1 - f_2^2(\cdot)_2}{f_1^2 - f_2^2} \\
(R)_{IF,s} &= x - x_{s2} + c\left(\delta t - \delta t_s\right) + T_s + (\varepsilon)_{(IF,s)} \\
(\Phi)_{IF,s} &= \left\| x - x_s \right\|_2 + c\left(\delta t - \delta t_s\right) + T_s + (\lambda A)_{IF,s} + (\lambda)_{IF,s} \, w_s + (\epsilon)_{IF,s} \\
T_s &= Z_h m_{h,s} + Z_w m_{w,s}
\end{aligned}
\tag{2}
$$

Note that the first equation defines the operator for the iono-free linear combination which is applied to the different terms. The dry zenith delay is computed using the receiver position whereas the wet zenith delay is estimated in the Kalman filter.

The Kalman state X consists of the receiver position x, velocity v, receiver clock offset $c\delta t$, receiver clock drift $c\dot{\delta}t$, wet zenith delay Z_w and the float ambiguities $(\lambda A)_{IF}$. We assume a constant velocity and constant clock drift for the state transition. With N_G being the number of GNSS and N_A the number of float ambiguities, this can be summarised as:

$$X^{t+\tau} = F(\tau)X^t = \begin{pmatrix} I_3 & \tau I_3 & & & & \\ & I_3 & & & & \\ & & I_{N_G} & \tau I_{N_G} & & \\ & & & I_{N_G} & & \\ & & & & 1 & \\ & & & & & I_{N_A} \end{pmatrix} \begin{pmatrix} x^t \\ v^t \\ c\delta t^t \\ c\dot{\delta}t^t \\ Z_w^t \\ (\lambda A)_{IF} \end{pmatrix} \quad (3)$$

We included the clock drift since it is a by-product of the velocity estimation described in subsection 4.2 and also allows for accurate prediction of receiver clock offset as the drift is quite stable over time. Furthermore, this can be used to have an accurate a priori estimate of the receiver clock offset even in case of a clock jump. For our JAVAD DELTA-3 and TRIUMPH-1M receivers the clock offset can have values up to ± 0.5 ms. If a clock jump is detected an accurate a priori clock offset can be obtained as follows:

$$c\delta t^{t+\tau} = c\delta t + \tau c\dot{\delta}t^t \pm c \cdot 0.001\,\text{s} - 0.001\,\text{s} \cdot c\dot{\delta}t^t$$

A receiver clock jump is detected by comparing the a priori estimate to either an SPP solution or by calculating a least squares fit of the clock offset from the a priori Kalman state and the code observations. Here, it is assumed that the position change and the sum of all the other errors is far less than 300 km which is the approximate size of a clock jump.

Figure 4. Histogram for difference of a priori and a posteriori clock offset for a 24 hour measurement campaign, 1 Hz, median receiver clock drift of about -692.86 m/s

In Figure 4 we can see that epochs with clock jumps (red bins) have a similar Gaussian white noise behavior with regards to the difference of a priori and a posteriori clock offset as all the other epochs (yellow bins) if the clock drift is considered. If the clock drift is not considered (blue bins), the difference will not have a mean of zero in epochs with a clock jump. As the estimates using (4) are as good as the a priori estimates in epochs without a clock jump, a reset of the uncertainties of the clock offset for the Kalman state is not needed.

4.2 Considerations for accurate velocity estimation

As described in Table 2 of section 2, we have tight requirements on the GNSS based position as well as on the velocity when entering a waterway lock. To guarantee a high accuracy in the velocity estimation as well as having a low uncertainty in the Kalman Filter which can then be used for the automatic steering, further thoughts have to be put into the velocity determination.

If we derive the velocity just by using the Kalman Filter as described in (3), the uncertainty of velocity will mostly depend on the trust in the state-transition model with regards to position and velocity. This has the disadvantage that if the velocity changes from one epoch to another, then the a priori estimate will be off and if additionally, too much trust is put into the state-transition, the a posteriori velocity will be off as well. On the other hand, if we put little trust into (3), then the uncertainty of the velocity in the Kalman filter will always be high regardless of its actual accuracy which would imply that the automatic steering cannot trust the PPP velocity.

Another way to estimate the velocity is using Doppler measurements which have an accuracy of a couple of cm/s [14], i.e. worse than the accuracy derived by (3) in case the constant velocity assumption holds. Nonetheless, it has the advantage of estimating instantaneous velocity without requiring any information from previous epochs. Therefore, we use them to have an a priori estimate of the velocity and clock drift in the first epoch or in case of a full reset of the Kalman filter. Otherwise, they are not used in our algorithm at all.

A third method are the time-differenced carrier phase measurements (TDCP) [3] which allow for calculating the relative change in position between two epochs. They are known [14] to have an accuracy of less than 1 cm/s without having to determine the ambiguities of the phase observations as long as they are constant for the two epochs considered. Therefore, cycle slip detection is of upmost importance as phase observations with cycle slips must be discarded for the computation of the TDCP and in the Kalman filter as well. As cycle slip detectors we use the Melbourne-Wübbena linear combination [1] and the geometry-free linear combination [15].

$$\frac{\Phi_{i,s}^{t+\tau} - \Phi_{i,s}^{t+\tau}}{\tau - c\delta t^t} \approx \frac{x^{t+\frac{\tau}{2}} - x_s^{t+\frac{\tau}{2}}}{\left\| x^{t+\frac{\tau}{2}} - x_s^{t+\frac{\tau}{2}} \right\|_2} \cdot \left(v^{t+\frac{\tau}{2}} - v_s^{t+\frac{\tau}{2}} \right) + c\dot{\delta}t^{t+\frac{\tau}{2}} \quad (5)$$

Note that (5) is abbreviated and also includes the time difference for the satellite clock offset, the tropospheric and the ionospheric delay from (1). For the delays we use the models from Saastamoinen [12] and Klobuchar [7]. In the real-time application the appropriate SSR corrections will be used. In case a receiver clock jump occurs, ± c·0.001 s has to be added in the nominator on the left-hand side of (5). Should computation time be a critical point in the real-time application, we found that it suffices to use linear interpolation to estimate the intermediate satellite position x_s and velocity v_s without having a significant

impact on the accuracy. The unknown receiver velocity v and clock drift $c\dot{\delta}t$ are calculated using a weighted least squares fit with the weights being the inverse of the sum of the noises of the phase observations in the Kalman filter divided by the time difference of the epochs.

$$\omega_{TDCP,s}^2 = \frac{100\left(\tau - c\dot{\delta}t^t\right)}{\sin^{-2}\alpha_s\left(t+\tau\right) + \sin^{-2}\alpha_s\left(t\right)}$$

Here, $\alpha_s(t)$ is the elevation angle of satellite s at time t. For GLONASS satellites the weights are divided by five. The weights imply that the values derived from (5) depend on the sampling frequency and will be worse with higher sampling frequency. On the other hand, the approximation error of the constant velocity model (3) will decrease. The optimal sampling rate is up for discussion which has to consider the requirements of the automatic steering. The accuracy of the TDCP with regards to the sampling frequency will be examined in section 5.

Once computed the a priori state estimates for the Kalman filter are as follows:

$$x^{t+\tau} = x^t + \tau v^{t+\frac{\tau}{2}}$$

$$v^{t+\tau} = v^{t+\frac{\tau}{2}}$$

$$c\delta t^{t+\tau} = c\delta t^t + \tau c\dot{\delta}t^{t+\frac{\tau}{2}} \qquad (7)$$

$$c\dot{\delta}t^{t+\tau} = c\dot{\delta}t^{t+\frac{\tau}{2}}$$
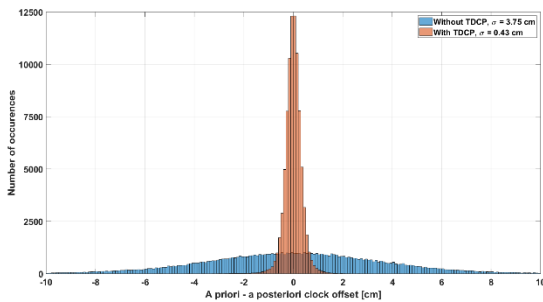
Figure 5. Histogram for difference of a priori and a posteriori clock offset for a 24 hours measurement campaign, 1 Hz, with and without TDCP

As can be seen in Figure 5 the inclusion of TDCP in the state-transition allows for a more accurate prediction of the clock offset which decreases the noise of the a priori residuals. This can be helpful in detecting outliers or cycle slips in the phase observations. Note that Figure 4 was produced without using those new a priori values based on TDCP.

5   RESULTS

For a measurement campaign associated with the SCIPPPER project a vessel, the MS NAAB in Regensburg as displayed in Figure 6, was equipped

with two antennas which were connected to a JAVAD DELTA-3 and a JAVAD TRIUMPH-1M receiver. Note that for this campaign the antennas were not mounted at the stern and bow of the vessel. In future measurement campaigns of the project it is planned to mount the antennas as described in section 2. Furthermore, RTCM SSR corrections were recorded which can later be used for the real-time algorithm development. As explained in section 4, in the following final products are used for the determination of precise satellite clock and orbits in our PPP algorithm. Unless stated otherwise we use observations from GPS, GLONASS and Galileo.

Figure 6. MS NAAB with two GNSS antennas (red circles) mounted on top

As a first accuracy test, we check the position difference of our postprocessing algorithm and the Canadian service in a quasi-stationary environment, that is the vessel was attached to a small pier as depicted in Figure 6. Therefore, the position is not fixed as there is influence from the current, the water level and the wind. As a reference we took the position calculated by the Canadian Spatial Reference System (CSRS) Precise Point Positioning service [17] at 4 a.m. and compare it to positions calculated between 0:00 and 4:00. The results can be seen in Figure 7.
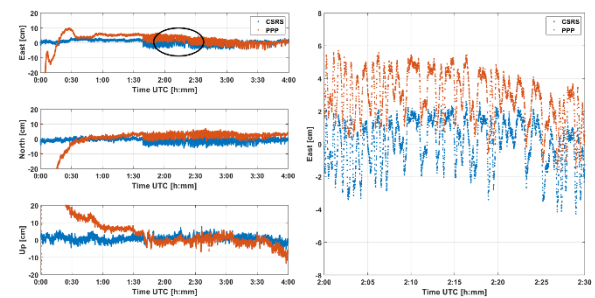
Figure 7. Portside antenna position difference with regards to CSRS position at 04:00, Regensburg, 25th of September 2019; Right-hand side: Zoom in of East component between 2:00 and 2:30 marked by black ellipsis on left-hand side

With regards to convergence we can see that it takes about 12 minutes in the East and 23 minutes in the North component until we have an estimated accuracy of less than 10 cm. The Up component takes about 51 minutes to reach the same levels of accuracy. In both algorithms we observed the same current motions in the East and North component starting from 1:40 a.m. which are emphasised on the right-hand side of Figure 7 though there seems to be a slight

offset of a couple of cm in the North and partially the East direction between the two PPP methods. In general, once the floating ambiguities have converged the results are at an acceptable level and lie in the requirements as mentioned in section 2.
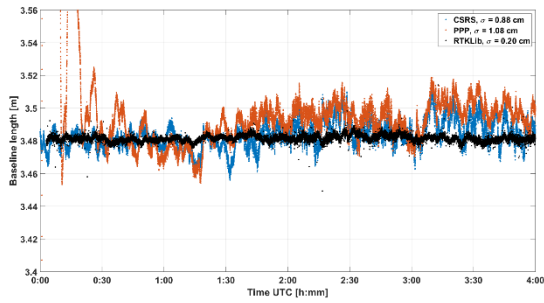
Figure 8. Baseline length of the two antennas in Regensburg campaign in the first four hours of 25th of September 2019; Standard deviation calculated for baseline between 1:00-4:00

As the vessel was equipped with two antennas, we can do an integrity test by comparing the baseline between the antennas. As a reference we used the RTKLib [16] software package in the differential "Moving-Base" positioning mode. In Figure 8 we can see that after about 45 minutes the baseline length derived from the PPP algorithms are quite similar though our method has a slight offset compared to the RTKLib reference and calculates a longer baseline length. In both methods the root-mean-square error (RMSE) with regards to the median solution from RTKLib considering all epochs between 1:00 and 4:00 is less than 2 cm. Therefore, both methods show a sufficient accuracy. The higher RMSE and variance of our postprocessing algorithm can be explained by the use of the iono-free linear combination which is known to increase the noise of the code and phase observations [15]. Furthermore, we only estimate float ambiguities instead of the integer ambiguities of (1) which can be fixed by introducing phase biases and using algorithms such as the LAMBDA method [18]. Furthermore, as our algorithms are developed with real-time application in mind, we cannot use methods such as a backward Kalman Filter which would help in finding cycle slips as well as improving the results in the first hour.
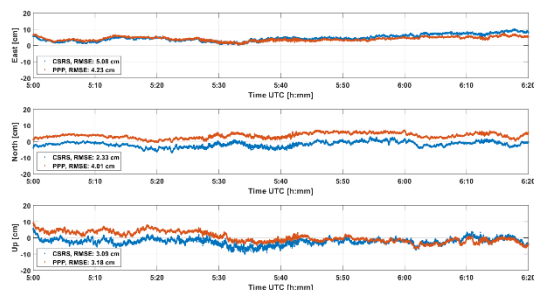
Figure 9. Position difference with regards to RTK reference of starboard antenna, 25th of September 2019

The second scenario considered is a dynamic one where the vessel is leaving the pier. As a reference we used Real Time Kinematic (RTK) by taking observations from a virtual reference station computed from several IGS stations which is two kilometres away from the position of the vessel at 5:00. The MS NAAB then moves in the direction of the reference station. We can see in Figure 9 that there is only a couple of a cm difference between the two PPP methods with our algorithm being closer to the RTK solution in the East component whereas the Canadian service is better in the North component. Note that the calculation started prior to 5 a.m. to allow our PPP algorithm to converge.
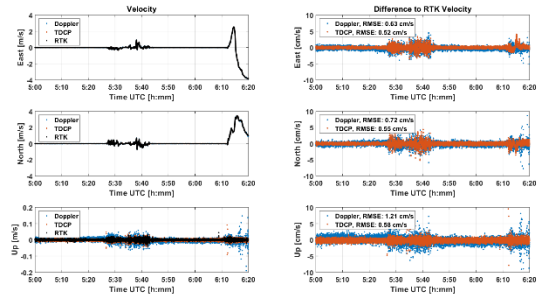
Figure 10. Left-hand side: Velocity of starboard antenna, 25th of September 2019; Right-hand side: Difference to velocity derived from RTK Position

Besides the position, the velocity is of high interest for the advanced driving assistance functions. Figure 10 shows the velocity in East (E), North (N), Up (U) for the dynamic scenario. We can see that the TDCP derived velocity is closer to the RTK solution than the one calculated from the Doppler measurements regardless whether we have a quasi-stationary or a dynamic scenario. Note that in the JAVAD receivers the Doppler smoothing bandwidth was set to 3 Hz which is the default value to avoid noisy velocity without having latency problems [8]. If we take a look at the velocity in the up direction on the left-hand side of the figure, the TDCP velocity is quite close to the RTK solution and it can be difficult to deduce what is the better solution of the two. To make a more accurate assertion of the accuracy, we will consider a static scenario where we have a reference velocity in all directions of zero.
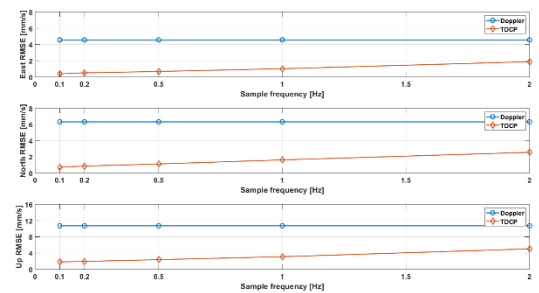
Figure 11. RMSE of Doppler and TDCP derived velocity for different sampling frequencies, 28th of August 2019, Neustrelitz

As a stationary scenario we used the GNSS measurements of an antenna which was mounted on the roof of the Institute of Communication and Navigation of the German Aerospace Center (DLR) in Neustrelitz, Germany. To consider different sampling frequencies, the measurements were downsampled from 2 Hz to 1 Hz, 0.5 Hz, 0.2 Hz and 0.1 Hz. The results of three hours of data can be seen in Figure 11

and Table 3. To make a fair comparison between the different sampling frequencies we only analysed the results of the common epochs, i.e. the measurements of every 10 seconds.

Table 3. RMSE of 3d velocity [mm/s] with regards to different sampling frequencies, 28th of August 2019, Neustrelitz

	0.1 Hz	0.2 Hz	0.5 Hz	1 Hz	2 Hz
Doppler	13.25	13.25	13.25	13.25	13.25
TDCP	2.00	2.19	2.72	3.66	5.96

We can see that the accuracy of the TDCP velocity is far better than the one derived from the Doppler measurements, especially for low sampling frequencies, and it seems to scale linearly with the sampling frequency with regards to the RMSE of the different ENU velocities. The Doppler results are the same for all epochs as the calculated velocity is instantaneous and does not depend on prior data and the time between epochs like the TDCP. While we do not have a reference at millimetres-per-second-level for the dynamic scenario shown in Figure 10, we are confident that the accuracy of the TDCP derived velocity is in the same regime as the algorithms used for both scenarios are identical. All in all, the time-differenced carrier phase measurements provide an accurate way to estimate the a priori velocity in a Kalman filter without requiring the convergence of ambiguities as long as we are able to detect cycle slips.

6 CONCLUSIONS AND FUTURE WORK

In this paper we presented the current status of our PPP algorithm which will be used for advanced driver assistance functions for inland waterway navigation. Here, the focus was on the bridge height warning system and the automatic passing of a waterway lock which lead to very stringent requirements on determination of position, orientation and velocity of the vessel. The requirements were deduced in the paper and overall system concept was described. The currently developed PPP algorithm, which is in detail described in the paper, shows an acceptable accuracy of the horizontal position of 10 cm which lies within the requirements of the driver assistant functions but the convergence time needs to be improved for real-time application. This will be done by using real-time SSR corrections which also allow for fixing the integer ambiguities. Besides the position, we have shown a highly accurate way to determine the velocity of the vessel at a millimetres-per-second-level even without knowing the ambiguities which, apart from the position and heading, is crucial for entering a waterway lock. We aim to conclude the development of the real-time PPP algorithm and also plan to fuse GNSS with IMU data which can help with potential GNSS errors or outage when passing a bridge.

As the next step within the project SCIPPPER the individual technology developments need to be finalised. These are the global PPP based positioning, the local positioning by using LIDAR, the automatic steering of the vessel and the new communication channel by using VDES. Finally, the system will be tested and validated with all components working together and a demonstration (see [13]) of the full system on the Main-Danube channel will be organised.

REFERENCES

1. Blewitt, G.: An Automatic Editing Algorithm for GPS data. Geophysical Research Letters. 17, 3, 199–202 (1990). https://doi.org/10.1029/GL017i003p00199.
2. Boehm, J., Schuh, H.: Vienna Mapping Functions. Presented at the 16th EVGA Working Meeting , Leipzig, Germany (2003).
3. Freda, P., Angrisano, A., Gaglione, S., Troisi, S.: Time-differenced carrier phases technique for precise GNSS velocity estimation. GPS Solutions. 19, 2, 335–341 (2015). https://doi.org/10.1007/s10291-014-0425-1.
4. Geo++: State Space Representation Format (SSRZ), http://www.geopp.de/wp-content/uploads/2020/09/gpp_ssrz_v1_0.pdf, last accessed 2021/01/12.
5. Hesselbarth, A., Medina, D., Ziebold, R., Sandler, M., Hoppe, M., Uhlemann, M.: Enabling Assistance Functions for the Safe Navigation of Inland Waterways. IEEE Intelligent Transportation Systems Magazine. 12, 3, 123–135 (2020). https://doi.org/10.1109/MITS.2020.2994103.
6. IALA: IALA: G1139 - ed.3 the technical specification of VDES. (2019).
7. J. A. Klobuchar: Ionospheric Time-Delay Algorithm for Single-Frequency GPS Users. IEEE Transactions on Aerospace and Electronic Systems. AES-23, 3, 325–331 (1987). https://doi.org/10.1109/TAES.1987.310829.
8. JAVAD GNSS: GNSS Receiver External Interface Specification. (2021).
9. Ma, H., Zhao, Q., Verhagen, S., Psychas, D., Liu, X.: Assessing the Performance of Multi-GNSS PPP-RTK in the Local Area. Remote Sensing. 12, 20, (2020). https://doi.org/10.3390/rs12203343.
10. Psychas, D., Verhagen, S.: Real-Time PPP-RTK Performance Analysis Using Ionospheric Corrections from Multi-Scale Network Configurations. Sensors. 20, 11, (2020). https://doi.org/10.3390/s20113012.
11. Raulefs, R.: Cellular VHF Data Exchange System. In: OCEANS 2019 MTS/IEEE SEATTLE. pp. 1–5 (2019). https://doi.org/10.23919/OCEANS40490.2019.8962676.
12. Saastamoinen, J.: Atmospheric Correction for the Troposphere and Stratosphere in Radio Ranging Satellites. In: Henriksen, S.W., Mancini, A., and Chovitz, B.H. (eds.) The Use of Artificial Satellites for Geodesy. pp. 247–251 American Geophysical Union (AGU) (1972). https://doi.org/10.1029/GM015p0247.

13. SCIPPPER: Schleusenassistenzsystem basierend auf PPP und VDES für die Binnenschifffahrt: http://scippper.de/, last accessed 2021/04/01.
14. Soon, B.K.H., Scheding, S., Lee, H.-K., Lee, H.-K., Durrant-Whyte, H.: An approach to aid INS using time-differenced GPS carrier phase (TDCP) measurements. GPS Solutions. 12, 4, 261–271 (2008). https://doi.org/10.1007/s10291-007-0083-7.
15. Subirana, J.S., Zornoza, J.M.J., Hernández-Pajares, M.: GNSS Data Processing, Vol. I: Fundamentals and Algorithms. ESA Communications (2013).
16. Takasu, T., Yasuda, A.: Development of the low-cost RTK-GPS receiver with an open source program package RTKLIB. Presented at the International Symposium on GPS/GNSS , International Convention Center Jeju, Korea (2009).
17. Tétreault, P., Kouba, J., Héroux, P., Legree, P.: CSRS-PPP: AN INTERNET SERVICE FOR GPS USER ACCESS TO THE CANADIAN SPATIAL REFERENCE FRAME. Geomatica. 59, 1, 17–28 (2005). https://doi.org/10.5623/geomat-2005-0004.
18. Teunissen, P.J.G.: The least-squares ambiguity decorrelation adjustment: a method for fast GPS integer ambiguity estimation. Journal of Geodesy. 70, 1, 65–82 (1995). https://doi.org/10.1007/BF00863419.
19. Wabbena, G., Schmitz, M., Bagge, A.: PPP-RTK: Precise Point Positioning Using State-Space Representation in RTK Networks. Presented at the Proceedings of the 18th International Technical Meeting of the Satellite Division of The Institute of Navigation (ION GNSS 2005) , Long Beach, CA (2005).
20. Zumberge, J.F., Heflin, M.B., Jefferson, D.C., Watkins, M.M., Webb, F.H.: Precise point positioning for the efficient and robust analysis of GPS data from large networks. Journal of Geophysical Research: Solid Earth. 102, B3, 5005–5017 (1997). https://doi.org/10.1029/96JB03860.